

Interpolymer Complexation of Poly(acrylic acid) and Poly(acrylamide): Structural and Dynamic Studies by Solution- and Solid-State NMR

Fred O. Garces,[†] K. Sivadasan,[‡] P. Somasundaran,[‡] and Nicholas J. Turro^{*}

Department of Chemistry, Columbia University, New York, New York 10027

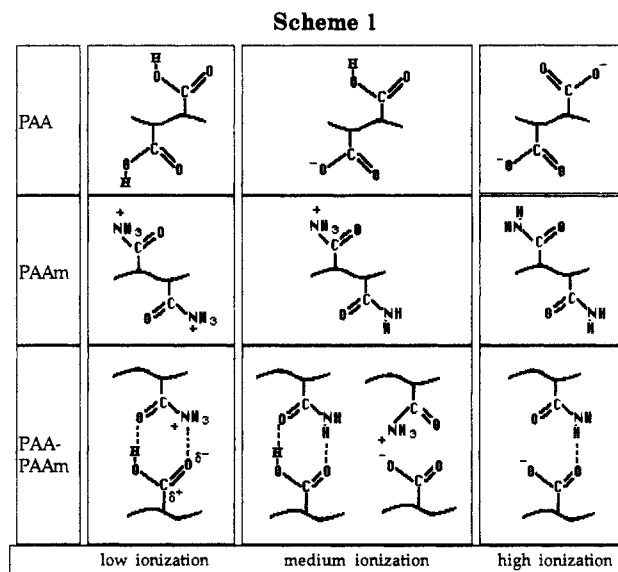
Received April 22, 1993; Revised Manuscript Received August 31, 1993[⊙]

ABSTRACT: Interpolymeric complexes of poly(acrylic acid) (PAA) and poly(acrylamide) (PAAm) at 60, 20, 5, and 0% ionization (α) were studied by $^1\text{H}/^{13}\text{C}$ solution-state and ^{13}C solid-state cross-polarization magic angle spinning (CPMAS) NMR experiments. The solid-state NMR results support a model in which ionization (α or pD) alteration leads to conformation and segment changes along the PAA-PAAm polymeric backbone. Solid-state relaxation measurements show short T_1 values at high ionization ($\alpha = 60\%$) but long T_1 values toward low ionization ($\alpha \leq 20\%$). This is consistent with a model in which the PAA and PAAm polymers take on a stretched but mobile conformation at high ionization but become immobile and restricted at low ionization. Dynamic restriction of the polymer is attributed to symbiotic hydrogen bonding of the carboxylic group of PAA and the amide residue of PAAm to form interpolymer complexes. Other relaxation parameters such as ^1H - ^{13}C cross-polarization times $T_{\text{CH}}(\text{SL})$, proton spin-lattice relaxation times in the rotating frame $T_{1\rho}(\text{H})$, and ^{13}C dipolar-dephasing results are also consistent with this model.

I. Introduction

Understanding the structure and dynamics of intermacromolecular complexes is of interest because of the occurrence of such structures in many systems of biological importance.^{1,2} The mechanism of complexation is an important prerequisite in predicting the microscopic structure and, through structure correlations, the macroscopic properties of these biopolymeric materials. Non-covalent binding forces derived from electrostatic, hydrogen bonding, and hydrophobic interactions have been attributed to be the main driving force for complexation of biopolymers.³⁻⁷ Investigations of the dynamics and structural characterization of these materials may provide insight into the macromolecular organization, which, in turn, may reflect the infrastructure and dynamics of the complexation mechanism at a molecular level.

Interpolymer complexation between poly(ethylene oxide) and poly(acrylic acid) has been characterized previously by NMR techniques,⁸ although only the polymer blend of poly(acrylic acid)-poly(acrylamide) (PAA-PAAm) has been studied by this technique.^{9,10} Interpolymer complexation between PAA and PAAm has previously been characterized by fluorescence measurements using pyrene-labeled PAAm (py-PAAm) fluorescence probes.^{11,12} The results were interpreted in terms of the occurrence of weak or negligible interactions for PAA and py-PAAm at $\text{pH} \geq 7.0$ and the occurrence of strong stable complexes at $\text{pH} \leq 4.5$ (shown in Scheme 1). This report describes the investigation by NMR spectroscopy of intermolecular complexes of PAA and PAAm for various degrees of ionization of PAA in a comparative manner. The modes of binding interactions, i.e., complexation of the carboxylic and amide residues, are monitored by NMR relaxation parameters. Although only



qualitative, the results of this study provide complementary but otherwise independent evidence on the cooperative binding nature of PAA-PAAm as reported previously by fluorescence techniques.^{11,12}

NMR relaxation techniques were used to monitor motions in the mid-kilohertz and megahertz frequency range, which may provide clues on the impact strength of these materials.¹³⁻¹⁶ The main mechanism for ^{13}C spin-lattice relaxation is due to ^1H - ^{13}C dipole-dipole interactions, with smaller contributions arising from chemical shift anisotropy and spin rotation.¹⁷ For low molecular weight polymers in the solution state, the spectral density offers a correlation time (τ_c) in the motional narrowing limit. In this limit, ($\omega \ll 1/\tau_c$), T_1 is inversely proportional to τ_c and is field independent. In the solid state, however, the spectral density yields $\omega^2\tau_c \ll 1$, and T_1 is directly proportional to τ_c and is field dependent.^{17,18} An indication of fast segment mobility, as it relates to the correlation times for these polymers, is therefore expected to yield large T_1 s in the solution state but small T_1 s in the solid state.^{19,20} In our experiments, NMR spectra were measured by a fast inversion-recovery pulse sequence, and

* Author to whom correspondence should be addressed.

[†] Department of Chemistry, University of San Diego, San Diego, CA 92110.

[‡] Henry Krumb School of Mines, Columbia University, New York, NY 10027.

[⊙] Abstract published in *Advance ACS Abstracts*, December 1, 1993.

the T_1 parameters were calculated by fitting the data to eq 1.

$$M(t) = M_1 \left\{ 1 - \left[2 - \exp\left(\frac{-\Delta}{T_1}\right) \right] \right\} \left[\exp\left(\frac{-t}{T_1}\right) \right] \quad (1)$$

$M(t)$ is the peak intensity as a function of time t , M_1 is the normalization constant, Δ is the delay time, and T_1 is the spin-lattice relaxation time.¹⁷⁻²¹

Two other relaxation techniques used here are (1) the variable spin-lock contact time experiment and (2) the dipolar-dephasing experiment.^{13-15,18-20,22-24} For (1), a varied contact time was added to the basic CPMAS pulse sequence. The results were fitted to eq 2.

$$M(t) = \frac{M_1}{1 - \left(\frac{T_{CH}}{T_{1\rho(H)}}\right)} \left\{ 1 - \exp\left(-\left[1 - \left(\frac{T_{CH}}{T_1}\right)\frac{t}{T_{CH}}\right]\right) \right\} \times \left[\exp\left(\frac{-t}{T_{1\rho(H)}}\right) \right] \quad (2)$$

$M(t)$ is the signal intensity as a function of contact time t , M_1 is the normalization constant, $T_{CH}(SL)$ is the cross-polarization time constant during the spin-lock period, and $T_{1\rho(H)}$ is the proton spin-lattice relaxation time in the rotating frame.²²⁻²⁴ The former relaxation parameter probes the static H-C dipolar interaction, whereas the latter monitors the rates of proton spin diffusion.

In the dipolar-dephasing experiment, (2), a time delay is inserted in the carbon channel of the CPMAS experiment after the ^1H - ^{13}C spin-lock period.^{14,20,25} The integrity of the signals after this period probes both the direct C-H dipolar coupling for a given ^{13}C resonance and the diminution of this dipolar coupling due to segment dynamics. The parameters derived from these measurements can be interpreted in terms of the molecular motion of the polymer chains as a function of variables such as pH or ionization.

II. Experimental Section

A. Materials. Poly(acrylic acid) purchased from Polysciences was used without further purification with a manufacturer-specified molecular weight of $M_w \approx 90\,000$.

The poly(acrylamide) sample was kindly supplied by American Cyanamid and had a number-average molecular weight, M_n , of $\approx 12\,000$. The polymer was purified by reprecipitating from aqueous solution using acetone as a nonsolvent.

B. Preparation. (1) **Solution-State NMR Studies.** Polymer samples were prepared by dissolving dried polymers in D_2O . Solution spectra were taken at ambient temperature ($20 \pm 2^\circ\text{C}$) with chemical shifts referenced to TMS.

(2) **Solid-State NMR Studies.** Polymer solutions were prepared in triple-distilled water. Poly(acrylic acid) (PAA) was neutralized to various extents by adding a predetermined volume of standard sodium hydroxide solution. Equimolar (monomer moles) solutions of poly(acrylamide) and poly(acrylic acid) were mixed for about 24 h and subsequently freeze-dried to remove water completely. Solutions of poly(acrylic acids) neutralized to various extents were also freeze-dried.

Seven samples were prepared for the solid-state NMR studies: (1) PAAm, neutral; (2) PAA, degree of ionization (α) = 60%; (3) PAA, α = 0%; (4) PAA-PAAm, α = 60%; (5) PAA-PAAm, α = 20%; (6) PAA-PAAm, α = 5%; (7) PAA-PAAm, α = 0%. The pDs of the samples before freeze-drying were 7.0, 4.75, 3.88, and 3.5 for α = 60, 20, 5, and 0%, respectively.

C. Instrumentation. Solution- and solid-state NMR measurements were acquired by a Bruker AF-250 FT-NMR spectrometer, and the spectra were recorded on an HP 5890A digital plotter. Detailed experimental conditions are described in a previous report.²⁶

D. Solid-State NMR. Each sample (ca. 250 mg) described above was packed in a 7-mm-o.d. sapphire (Al_2O_3) rotor with Kel-F end caps (Doty Scientific). The high-power preamplifier for the CPMAS experiment was provided by IBM instruments, and the probe was designed by Doty Scientific. Carbon-13 cross-polarization magic angle spinning with high-power heteronuclear decoupling, ca. 40 kHz, was used to obtain high-resolution NMR spectra. The dipolar-dephasing, pulse sequence experiment provided proton-decoupled carbon resonance assignments. In this experiment, a 50- μs dephasing period was used. The CPMAS experiment consisted of matching the Hartmann-Hahn condition [$(\gamma B_1)_C = (\gamma B_1)_H$], contact times of 1500-2000 μs , a pulse width for ^1H of 5.8 μs , and recycled delays between 2 and 5 s (6 s for ^{13}C T_1 measurements). Spinning rates were between 3 and 5 kHz, and chemical shifts were referenced to the methyl carbon of external hexamethylbenzene (Me, δ = 16.7 ppm vs TMS). All measurements were taken at ambient temperature (20°C).

Spin-lattice relaxation times for ^{13}C nuclei were measured by the fast inversion-recovery pulse sequence (90° - ^1H spin lock, ^{13}C contact)- 90° - τ - 90° -fid). All T_1 measurements were performed at room temperature. Recycled delays were set to 6 s (ca. $(3-4) \times T_1$), with delay times of 0.05, 1.0, 5.0, 15.0, 45.0, and 120.0 s. In some instances, however, delay times up to 320 s were used. T_1 s from the measured ^{13}C spectra were calculated by the Bruker spectrometer Aspect 3000 computer and confirmed by curve-fitting routines (KaleidaGraph 2.1.3 for the Macintosh). Other pulse programs included variable spin-lock contact times and variable dipolar-dephasing experiments. In the polarization transfer spin-lock experiment, contact times between 50 and 6000 μs were used; the resulting signal intensities from the ^{13}C NMR spectra were curve fit in KaleidaGraph to determine the rise time $T_{CH}(SL)$ and decay period $T_{1\rho(H)}$ of the carbon signal intensities.

III. Results and Discussion

A. Solution-State NMR. In the literature, tacticity analyses have been made for polyacrylates based on ^1H and ^{13}C NMR results.²⁷⁻³³ For our experimental conditions (20°C), only triad sensitivity could be observed at best. Figure 1, shows the ^1H NMR spectra of (a) PAAm in D_2O under neutral conditions, (b) PAA at pD = 3.5, (c) PAA at pD = 7.0, (d) PAA-PAAm at pD = 3.5, and (e) PAA-PAAm at pD = 7.0. These spectra all show a pD dependence with significant resonance line broadening (line width, $W_{1/2} > 40$ Hz). Despite the occurrence of line broadening, resonance assignments are readily made based on the integrated area of the signals by literature comparison^{27,28,31,34,35} or by computer simulation analysis.³⁶⁻⁴¹ For PAAm in D_2O (Figure 1a) the broad resonance centered at 2.08 ppm is assigned to the α -protons and the resonance at 1.53 ppm is assigned to the β -protons of the monomer unit, which are consistent with the 1:2 integration. The tacticity of PAAm has previously been assigned as a mixture of isotactic and syndiotactic species based on ^1H NMR methods.²⁸ Our result is not consistent with this but representative of a more complicated microstructure which will be discussed in the context of the ^{13}C NMR result.

The ^1H NMR spectrum for PAA at pD = 3.5 (Figure 1b) shows a more complicated resonance pattern with four distinct resonances centered at δ = 2.26, 1.80, 1.63, and 1.52 ppm; weaker signals are observed at 2.65, 1.97, and 1.50 ppm. The three resonances between 1.50 and 1.80 ppm are assigned to the β -protons, and the 2.26 ppm resonance is assigned to the α -proton. Previous tacticity analysis of PAA at pH = 2 is consistent with our result here in which the triad distribution of the *rr*, *mr*, and *mm* sequences is assigned to the methylene resonances at 1.80, 1.63, and 1.52 ppm, respectively.^{27,28} At pD = 7.0, the PAA ^1H NMR spectrum shows two broad resonances centered at 1.96 (α -proton) and 1.39 ppm (β -protons),

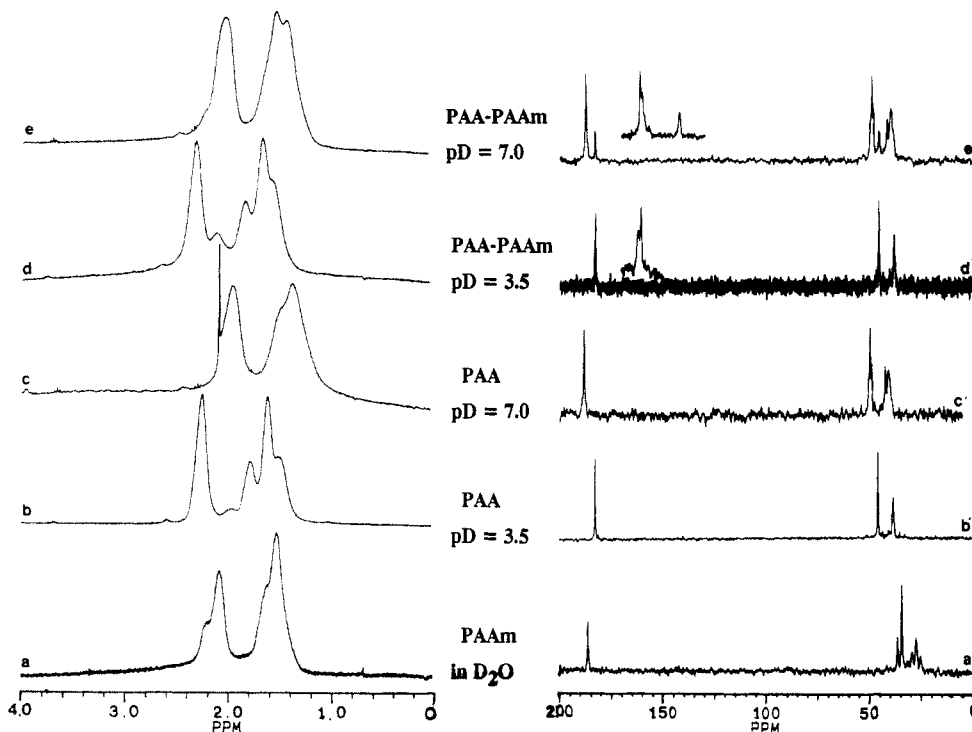


Figure 1. ^1H (a–e, left) and ^{13}C (a'–e', right) solution-state NMR spectra in D_2O vs TMS for (a) PAAm, (b) PAA at pD = 3.5, (c) PAA at pD = 7.0, (d) PAA-PAAm at pD = 3.5, and (e) PAA-PAAm at pD = 7.0.

(Figure 1c). Tacticity assignment based on the ^1H NMR results is difficult at this point because of the poor resolution of the signals. The sharp signal at 2.10 ppm is assigned to adventitious acetone.

A mixture of PAA and PAAm at pD = 3.5 (Figure 1d) shows a ^1H NMR spectrum similar to that of the PAA ^1H NMR spectrum at pD = 3.5 (Figure 1b). Proton resonances from the spectrum in Figure 1d indicate a downfield shift of the resonance at 2.26–2.31 ppm but otherwise minor differences in the chemical shifts of the other signals at 2.11, 1.83, 1.67, and 1.60 (shoulder) ppm. This ^1H NMR spectrum can be characterized as the sum of ^1H signals from the ^1H NMR spectra of PAA at pD = 3.5 (Figure 1b) and PAAm (Figure 1a). Tacticity assignment based on the methylene resonances is similar to those of PAA-PAAm at pD = 3.5.⁴² In comparison, the ^1H NMR spectrum for PAA-PAAm at pD = 7.0 (Figure 1e) shows broad structureless resonances at higher field ($W_{1/2}$ ca. 50 Hz): δ = 2.08 and 1.54/1.44 ppm. The ^1H assignments are analogous to the other assignments; the upfield resonances are assigned to the β -protons, and the downfield resonances are assigned to the α -proton. The chemical shifts are listed in Table 1.

The corresponding ^{13}C NMR spectra under various ionization conditions are shown in Figure 1a'–e'. The chemical shifts are given in Table 1. The NMR spectrum for PAAm in D_2O shows six resonances centered at 187.4 (C=O); 36.3, 34.3 (C_α); and 30.0, 28.1, 26.3 ppm (C_β) (Figure 1a'). Based on the carbonyl resonances, our PAAm sample is consistent with a homopolymer (<5% hydrolysis).^{9,10,29,30} The methine, C_α , resonances show only two signals, short of the triad sensitivity reported by Lancaster which was obtained at 70 °C.³⁰ The methylene resonances, C_β , are more diagnostic of triad sensitivity, however, with the 30.0 and 26.3 ppm signals assigned to the *rr* and *mm* configurations, respectively, and the 28.1 ppm signal assigned to the heterotactic (*rm* + *mr*) configuration.^{9,10,30} We make no attempts here to computer simulate these spectra to quantify the tacticity of the structure.

For PAA at pD = 3.5 (Figure 1b') the ^{13}C NMR spectrum shows carbon resonances at 182.4 (C=O); 45.2 (C_α); and

Table 1. ^1H and ^{13}C Chemical Shifts and Carbon-13 Spin-Lattice Relaxation Times (T_1) for PAAm, PAA, and PAA-PAAm Mixture at Various Ionizations (pD) vs TMS

	PAAm	PAA pD = 3.5	PAA pD = 7.0	PAA- PAAm pD = 3.5	PAA- PAAm pD = 7.0
C=O (ppm)	187.4	182.4	188.2	183.5 182.7	187.8 186.8 183.1
^{13}C T_1 (s)	—	2.8	2.2	1.4 1.4	1.8 1.8 1.4
H_α (ppm)	2.08	2.26	1.96	2.31	2.08
C_α (ppm)	36.3 34.3	45.2	49.6 48.9	45.5	49.8 49.1 48.3 45.8
^{13}C T_1 (s)	—	0.2	0.3 0.2	0.2	0.2 0.2 0.2
H_β (ppm)	1.53	1.80 1.63 1.52	1.39	1.83 1.67 1.60	1.54 1.44
C_β (ppm)	30.0 28.1 26.3	38.5 37.9	42.3 40.6	38.0 38.1	41.8 40.0
^{13}C T_1 (s)	—	0.1 0.1	0.1 0.1	0.2 0.2	0.1 0.2

38.5, 37.9 ppm (C_β). Under less acidic conditions, pD = 7.0, the resonances broaden and shift downfield to 188.2 (C=O); 49.6, 49.0 (C_α); and 42.3, 40.6 (C_β) (Figure 1c'). Analysis of PAA by Chang consists of minimal fine structure at low pD.²⁷ Furthermore, Schaefer analysis of PAA consists of a syndio-, hetero-, and isotactic sequence at high pH but mostly isotactic sequence at low pH.³² A pure Bernoullian atactic sequence for PAA has been suggested by Truong, which is more consistent with our results.^{9,10}

The PAA-PAAm spectrum at pD = 3.5 (Figure 1d'), shows carbon resonances at 183.5, 182.7 (C=O); 45.5 (C_α); and 38.0, 38.1 ppm (C_β). At pD = 7.0 (Figure 1e') the ^{13}C

NMR spectrum for the PAAm-PAA polymeric mixture shows a more complicated chemical shift pattern. Resonances are observed at 187.8, 186.8, 183.1 (C=O); 49.8, 49.1, 48.3, 45.8 (C_α); and 41.8, 40.0 ppm (C_β). Essentially, the two carbonyls from PAA and PAAm are observed in this spectrum, whereas at lower pD, only the carbonyl from PAA is resolved, with the splitting of this resonance indicative of complexation between the carboxylic group of PAA and the amide group of PAAm.⁸

The ^{13}C T_1 spin-lattice relaxation times are listed in Table 1; measurements could not be obtained for PAAm in D_2O , owing to the excessive number of accumulations needed to obtain adequate signal-to-noise. The T_1 values for the carbonyl resonances for PAA at pD = 3.5 and pD = 7.0 (2.8 and 2.2 s, respectively) do not indicate any significant changes. This same trend (T_1 s of 1.4 and 1.8/1.4 s, respectively) is observed for the carbonyl resonance of PAA-PAAm at pD = 3.5 and pD = 7.0. The relaxation times for the carbon atoms of the aliphatic backbone show a similar behavior in which the T_1 s do not show any significant variation with pD changes.

Relaxation pathways for polymeric samples may be linked to a number of intermolecular processes; the interactive process of polymer complexation, a chain self-coiling mechanism,^{6,11,12,43} a pH effect on ionicity,^{4,31,42} tacticity,⁴⁴ residual H_2O ,⁴⁵ and/or segment conformational perturbation.²⁷ The trend-free T_1 relaxation results in Table 1 suggest that segment mobility is just one of many other mechanisms for relaxation in the solution state. Our results were not conclusive since these values show only minor deviation with little connection between long correlation times (short T_1 s) and restricted mobility at low pD.⁴³ These effects must be deconvoluted to arrive at any conclusion about mobility and relaxation time in the solution state.²¹ We make no attempts here, however, to quantify these contributions. Finally, the inconclusive result in solution-state studies of this work compared to that of the fluorescence work may be attributed to the difference in experimental conditions. The luminescence studies used dilute concentrations of the polymer, whereas the NMR solution-state measurements required higher concentrations to produce acceptable signal-to-noise. These and other differences in experimental conditions may have resulted in relaxation measurements more representative of ionization effects and concentration factors rather than conformation and mobility.

B. Solid-State NMR. The ^{13}C CPMAS and dipolar-dephasing (DD) spectra for samples of PAAm, PAA ($\alpha = 0, 60\%$), and PAA-PAAm ($\alpha = 0, 5, 20, 60\%$) are shown in Figure 2, with spectra a-g corresponding to the CPMAS spectra and spectra a'-g' corresponding to the dipolar-dephasing spectra. In general, the alkyl resonances, C_α and C_β , are broad and difficult to resolve. Based on the ^{13}C NMR assignment above and assignments of other polyacrylates in solution^{29-32,43} and the solid state,^{8,35,45} the intense signal downfield is assigned to the C_α resonance, with the shoulder upfield assigned to the C_β resonances. Chemical shifts are listed in Table 2 together with the spin-lattice relaxation times, T_1 . The ^{13}C CPMAS spectrum for PAAm under neutral conditions (Figure 2a), shows four resonances with the following assignments; C=O, 180 ppm; C_α , 51/42 ppm; and C_β , 37 ppm (shoulder).^{7,34} Under dipolar dephasing, the broad resonance centered at 42 ppm is suppressed, while the resonances at 180 and 51 ppm are affected only slightly.

Spectra 2b, b' and c, c' show the CPMAS and DD spectra for PAA at $\alpha = 0$ and 60% and are consistent with the CPMAS spectra obtained by Fyfe.³⁵ The dipolar-dephas-

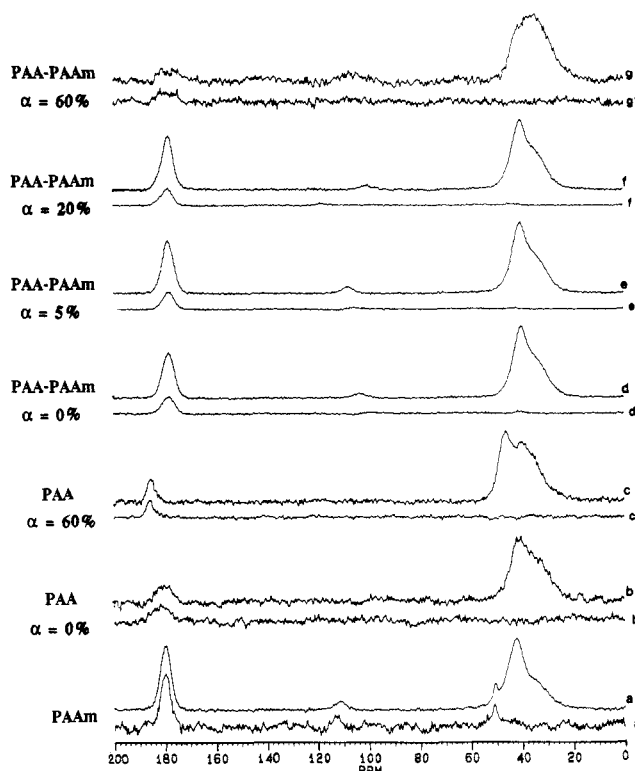


Figure 2. ^{13}C cross-polarization magic angle spinning (a-g) and dipolar-dephasing (a'-g') solid-state NMR spectra vs external hexamethylbenzene for (a) PAAm, (b) PAA at $\alpha = 0\%$, (c) PAA at $\alpha = 60\%$, (d) PAA-PAAm at $\alpha = 0\%$, (e) PAA-PAAm at $\alpha = 5\%$, (f) PAA-PAAm at $\alpha = 20\%$, and (g) PAA-PAAm at $\alpha = 60\%$.

ing spectra under these two conditions show the total suppression of the alkyl signals upfield (≈ 34 -45 ppm) and about a 30% suppression of the carbonyl signals. Furthermore, the ^{13}C resonances for $\alpha = 60\%$ are shifted ca. 5-7 ppm further downfield than those for $\alpha = 0\%$, while line broadening for the carbonyl at $\alpha = 60\%$ is not as severe as those at $\alpha = 0\%$. The chemical shift assignments for $\alpha = 0\%$ consist of C=O, 177 ppm; C_α 40 ppm; and C_β , 34 ppm, with line broadening of $W_{1/2} = 500$ Hz for the carbonyl and 1200 Hz for the alkyl resonances.^{7,14,27,35} Assignments for $\alpha = 60\%$ consist of C=O, 186 ppm; C_α 45 ppm; and C_β , 40 ppm.

The CPMAS spectra for the PAA-PAAm polymeric mixture at $\alpha = 0, 5,$ and 20% (Figure 2 d-f) all show similar spectral features. The carbonyl resonances are centered around 178 ppm, with the broad alkyl resonances ranging from 54 to 33 ppm; the C_α s are assigned to the signal centered at ≈ 40 ppm, whereas the C_β s are assigned to the shoulder at ≈ 34 ppm. Dipolar dephasing leads to the total suppression of the alkyl resonances and partial suppression of the carbonyl resonances. Line broadening of the carbonyl and alkyl resonances is unaffected by ionization changes.

Finally, the CPMAS spectrum of PAA-PAAm at $\alpha = 60\%$ (Figure 2g) shows poor signal-to-noise even after acquiring 4 times as many fids as those of the other polymeric samples. In the carbonyl region, there are at least two signals (181 and 177 ppm), while in the alkyl region (39 and 32 ppm) a broad Gaussian-like resonance appears. Although the spectrum is noisy, the dipolar-dephasing result is similar to the preceding three: total suppression of the alkyl carbon resonances and partial suppression of the carbonyl resonances. The ^{13}C chemical shifts are compiled in Table 2.

The broad resonances observed in the CPMAS result from distribution of chemical shifts due to steric con-

Table 2. Carbon-13 CPMAS NMR Chemical Shifts and Relaxation Times T_1 , $T_{CH}(SL)$, and $T_{1\rho}(H)$ for PAAm, PAA, and PAA-PAAm Polymers at Various Ionizations (α) vs External Hexamethylbenzene (Me, $\delta = 16.7$ ppm)

	PAAm	PAA $\alpha = 0\%$	PAA $\alpha = 60\%$	PAA-PAAm $\alpha = 0\%$	PAA-PAAm $\alpha = 5\%$	PAA-PAAm $\alpha = 20\%$	PAA-PAAm $\alpha = 60\%$
C=O (ppm)	180	177	186	178	179	178	181
T_1 (s)	37	18	13	44	37	33	177
$T_{CH}(SL)$ (μ s)	—	—	—	1406	932	1485	3138
$T_{1\rho}(H)$ (ms)	—	—	—	1.9	2.6	1.5	3365
C_α (ppm)	51	40	45	40	40	41	3.1
T_1 (s)	42	23–21	14–8	58	36	30	4.7
	5						39
	34						17
$T_{CH}(SL)$ (μ s)	—	—	—	98	104	124	300
$T_{1\rho}(H)$ (ms)	—	—	—	4.4	4.3	3.9	7.5
C_β (ppm)	37	34	40	34	33	34	32
T_1 (s)	31	14	6	30	26	14	6
$T_{CH}(SL)$ (μ s)	—	—	—	85	48	116	774
$T_{1\rho}(H)$ (ms)	—	—	—	3.7	4.2	4.0	5.5

straints limiting molecular motion in the solid state. In the solution state, random fluctuation of the polymer time-averages all possible arrangements, so that the chemical shift from the nuclear spins is averaged. However, in the solid state, conformations are frozen out with the chemical shift sampling all possible conformations. This situation is reflected in line broadening and the relaxation times, as discussed below.

As mentioned earlier, the PAAm CPMAS spectrum shows an anomalous resonance at 51 ppm which persists upon dipolar dephasing. Magnetization survival after a 50- μ s dipolar-dephasing period is associated with carbons having weak 1H - ^{13}C dipolar coupling because of inefficient polarization transfer, e.g., quaternary carbon, or rapid rotation along the C-H bond.^{14,20,25} We attribute the perseverance of the resonance of 51 ppm to the latter; i.e., the terminal segments of the PAAm backbone undergo rapid random fluctuation, causing ineffective H-C dipolar coupling.⁴⁶ With the exception of the PAAm, 51 ppm resonance, all other alkyl resonances are suppressed upon dipolar dephasing, suggesting that the motion involved along the polymeric backbone is not significant enough to diminish the H-C dipolar coupling.

Differences in line broadening and resolution in the CPMAS spectra of PAA at $\alpha = 0$ and 60% may originate from various stages of hydrogen bonding, ionic environment, and/or conformational arrangement as a result of the degree of ionization (α). At high ionization, the PAA possesses repulsive Coulombic interactions among the $-COO^-$ groups along the polymeric backbone which give rise to resolved C_α and C_β resonances.^{11,12,42} Moreover, ionization in the medium to low range (see Scheme 1) may contribute to different polymeric environments, giving rise to multiple signals, i.e., greater broadening.³⁵ For the PAA-PAAm CPMAS spectra at $\alpha = 0, 5,$ and 20%, the line broadening and resonance pattern are similar, in contrast to PAA-PAAm at $\alpha = 60\%$.

The T_1 values were determined for polymeric samples at various degrees of ionization. The signal intensities of the T_1 stacked plots were fitted to eq 1, and Figure 3 shows a representative curve fit for the C_α resonances of PAA-PAAm at $\alpha = 60, 20, 5,$ and 0%; the T_1 values are listed in Table 2. Carbon-13 T_1 relaxation values for PAAm (Table 2) fall between 31 and 37 s except for the anomalous resonance at 51 ppm, which possesses a T_1 of ca. 5 s. Short relaxation times for this resonance are consistent with a PAAm terminal group undergoing rapid fluctuation with correlation times in the order of the Larmor frequency (~ 60

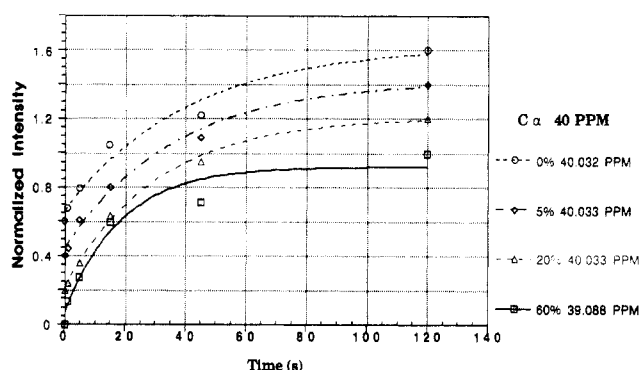


Figure 3. Plots of ^{13}C relative signal intensities versus delay times (s) for the CPMAS fast inversion-recovery pulse sequence experiment of the C_α resonance ($\delta \approx 40$ ppm) at $\alpha = 0, 5, 20,$ and 60%.

MHz). T_1 s for the other resonances in PAAm are longer than those of PAA at $\alpha = 0$ and 60%. The T_1 s for PAA at $\alpha = 0\%$ are 18 (177.3 ppm), 21–23 (40 ppm), and 14 s (34 ppm shoulder) and those for $\alpha = 60\%$ are 13 (186 ppm), 8–14 (45 ppm), and 6 s (40 ppm). It is noted that since the alkyl resonances overlap, the best T_1 estimates for C_α and C_β are a composite of the T_1 values for the overlapping signals. Because of severe line broadening of the signals in the CPMAS spectrum, the T_1 values are expected to have error limits of 20%.

For the PAA-PAAm polymeric mixture at $\alpha = 0, 5, 20,$ and 60%, the T_1 values decrease systematically as ionization increases. For example, at $\alpha = 0\%$, T_1 s for the C=O, C_α , and C_β resonances are 44, 58, and 30 s, respectively, while those at $\alpha = 60\%$ are 19/21, 17, and 6 s, respectively; T_1 values for PAA-PAAm at $\alpha = 5$ and 20% fall between these two limits.

The spin-lattice relaxation results suggest that the extent of ionization plays an important role on the conformation and motional behavior of the polymer. The T_1 results for PAAm show that the carbonyl resonance has a relaxation time similar to that of its C_α and C_β resonances (neglecting the 51 ppm resonance). This is consistent with PAAm nondependency on ionization effects. In comparison, the T_1 values of PAA at 60 and 0% do show a strong correlation to ionization changes. For example, between 60 and 0% ionization, the carbonyl relaxation time increases by 38% (13 to 18 s), with a similar result for the alkyl resonances. The T_1 variation for PAA-PAAm also shows a similar trend with more pronounced differences. A more detailed study would involve decon-

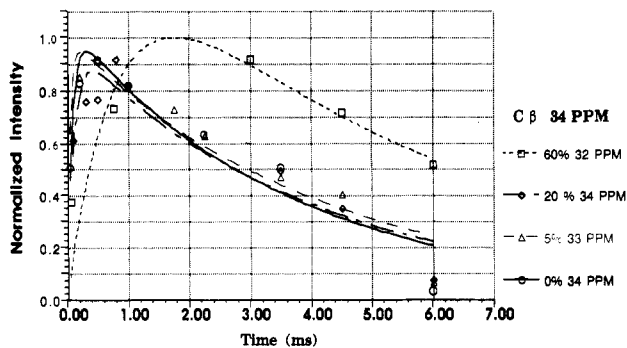


Figure 4. Plots of ^{13}C relative signal intensities versus contact times (ms) for the variable contact time CPMAS pulse sequence experiment of the C_β resonance ($\delta \approx 34$ ppm) at $\alpha = 0, 5, 20,$ and 60% .

volution of the other relaxation factors by a variable-temperature study, but, qualitatively, the results discussed below are sufficient to describe the interpolymer complexation process.

Qualitative analysis of the T_1 result for the interpolymer PAA-PAAM complexes must take into consideration contributions due to ionization effects and segment mobility.⁴⁷ If the T_1 result for the homopolymer PAA is used as a baseline reference for the contribution due to ionization effects and other relaxation mechanisms, then differences between the two systems, homopolymer PAA and interpolymer complexes PAA-PAAM, should reflect contributions only due to segment dynamics as a result of complexation. The T_1 results in Table 2 show a large deviation between the two ionization limits for PAA-PAAM compared to that of PAA. Qualitatively, all else being equal, we attribute the increase of T_1 at lower ionization ($\alpha = 0\%$) for the PAA-PAAM system relative to the homopolymer PAA system to the longer correlation times associated with the complexation process, thereby restricting the segment mobility of the interpolymer complex.^{14,18}

Contact times ranging from 50 to 6000 μs were used for the variable contact time experiment of PAA-PAAM at $\alpha = 60, 20, 5,$ and 0% . Figure 4 shows a representative ^{13}C magnetization buildup and decay for the C_β resonances with $T_{\text{CH}}(\text{SL})$ and $T_{1\rho}(\text{H})$ values listed in Table 2. The results show that maximum magnetization polarization is approached fastest for $\alpha = 0\%$ and slowest for $\alpha = 60\%$. Magnetization buildup depends on the strength of the C-H dipolar interaction, which is also influenced by molecular mobility between the two dipoles.^{13-16,18-20,22,48} The rapid growth of the ^{13}C signals, short $T_{\text{CH}}(\text{SL})$, at lower ionization therefore is diagnostic of the strong C-H dipolar interaction as a result of restricted mobility, while the longer $T_{\text{CH}}(\text{SL})$ values at high ionization are consistent with rapid segment dynamics, resulting in weak C-H dipolar coupling. Thus our relaxation results suggest that the polymeric chain undergoes rapid contortion at high ionization ($\alpha = 60\%$), resulting in less efficient cross-polarization of the abundant ^1H spins to the rare ^{13}C spins but restricted mobility of the chain at lower ionization ($\alpha = 0\%$), yielding strong H-C dipolar coupling, and efficient ^1H to ^{13}C polarization transfer. This systematic trend for the $T_{\text{CH}}(\text{SL})$ values under the different ionization conditions shown in Table 2 is in agreement with the spin-lattice relaxation result and polymeric model established by the fluorescence study.

Finally, the $T_{1\rho}(\text{H})$ values for these samples do not show significant variation for the different ionization conditions, suggesting that polymeric chain dynamics are not near the 40-kHz domain of the spin-locking field used in the

experiment and further that the proton spin diffusion has equilibrated.

IV. Conclusions

The interaction between two polymers, PAA and PAAM, which undergo complexation has been investigated by NMR techniques in this report. The following summarizes the behavior of the interpolymer complexes as reflected by the NMR results. The average structure of PAAM does not have any pD dependence as suggested by the similarities of the T_1 values for the different resonances of PAAM. The average structure of PAA, on the other hand, is ionization dependent; at high pD or ionization, it exists in the ionized form which affects the polymeric backbone in two ways. First, the Coulombic repulsion tends to stretch the polymer segments, and as a result, this leads to the second effect, namely, rigidity of the polymer. We do not observe this in our relaxation results, however.

As the pD decreases or as α approaches zero, the ionized form of the carboxyl group becomes protonated. Less "ionized form" leads to less Coulombic interaction, which leads to the contraction of the polymeric segments and increased segment mobility. Our relaxation data suggest that at 60% ionization we are already in this regime of increased segment mobility. As the ionization decreases, H-bonding processes become operative and influential on the behavior of the polymer segments. At low enough ionization, the H-bonding network begins to accumulate due to the contraction of the polymers. Thus the contracted form now becomes immobile, and a point is reached in which the contracted form is less mobile than the extended form which exists at higher ionization. This picture of restricted mobility of the polymer segment is consistent with the systematic trend observed in both the T_1 and $T_{\text{CH}}(\text{SL})$ result.

When PAA and PAAM are mixed to form an interpolymer complex, there is a parasitic relationship; that is, PAA dictates the configuration of the complex. At high pD, the two polymers act independently and there is no interaction between the two polymers, but at low ionization, PAA is deionized and either can intramolecularly H-bond to itself or can intermolecularly H-bond to PAAM as reflected in the relaxation results. As the intermolecular interaction becomes efficient, the PAAM takes on properties associated with PAA.

For the homopolymer, the T_1 result will not only have contributions from the model discussed above but also have contributions from other factors such as the pD effect on ionicity, tacticity, and/or residual H_2O interaction. We use the relation results for this system to provide a reference point for the interpolymer complexation process. That is, if we compare the relaxation results of the homopolymer at the two extreme conditions, $\alpha = 60$ and 0% , to that of the interpolymer complexes under these same conditions, then we can qualitatively assert that the differences in the T_1 results are due to the segment dynamics of the latter. The results here indicate longer T_1 for the PAA-PAAM system at 0% ionization than that of PAA homopolymer, which is consistent with a more effective complexation process of PAA to PAAM. Interpretation of the $T_{\text{CH}}(\text{SL})$ result is consistent with this model.

In conclusion, the solid-state NMR studies of poly(acrylic acid) and poly(acrylamide) at various ionization support a polymer model in which at low levels of ionization the PAA-PAAM solutions form an interpolymer complex resulting in a relatively rigid polymeric mixture exhibiting

slow chain motions. At high levels of ionization, the PAA-PAAM complexes exist as random polymeric chains with rapid segment dynamics. Although the solution-state NMR studies were not conclusive, due to concentration effects or the nature of the H-bond in these materials, the solid-state CPMAS studies are consistent with the model established from fluorescence studies. Moreover, the results here show that interpolymer complexation is very strong in the solid state. Finally, the results demonstrate that CPMAS NMR is a powerful experimental technique for investigation of the effect of interpolymer complexation on segmental motion and macromolecular dynamics in the solid state.

Acknowledgment. The authors thank the NSF and DOE for their generous support of this research. They also thank Professor Miguel Garcia-Garibay for comments and discussion of the results.

References and Notes

- (1) Bekturov, E. V.; Bimendina, L. A. *Adv. Polym. Sci.* **1981**, *41*, 99.
- (2) Tsuchida, E.; Abe, K. *Adv. Polym. Sci.* **1982**, *45*, 1.
- (3) Nikolaev, A. F.; Shibalovich, V. G.; Perina, G. P.; Bondarenko, V. M. *Vysokomol. Soedin., Ser. B* **1976**, *18*, 222.
- (4) Abe, K.; Koide, M.; Tsuchida, E. *Macromolecules* **1977**, *10*, 1259.
- (5) Higashi, N.; Nojima, T.; Niwa, M. *Macromolecules* **1991**, *24*, 6549.
- (6) Bednar, B.; Li, Z.; Huang, Y.; Chang, L.-C. P.; Morawetz, H. *Macromolecules* **1985**, *18*, 1829.
- (7) Candau, F.; Zekhnini, Z.; Heatley, F. *Macromolecules* **1986**, *19*, 1895.
- (8) Maunu, S. L.; Korpi, T.; Linberg, J. J. *Polym. Bull.* **1987**, *18*, 172.
- (9) Truong, N. D.; Galin, J. C.; François, J.; Pham, Q. T. *Polymer* **1986**, *27*, 459.
- (10) Truong, N. D.; Galin, J. C.; François, J.; Pham, Q. T. *Polymer* **1986**, *27*, 467.
- (11) Sivadasan, K.; Somasundaran, P.; Turro, N. J. *Colloids Polym. Sci.* **1991**, *269*, 131.
- (12) Sivadasan, K.; Somasundaran, P.; *J. Polym. Sci., Part A: Polym. Chem.* **1991**, *29*, 911.
- (13) Schaefer, J.; Stejskal, E. O. High-Resolution ^{13}C NMR of Solid Polymers. In *Topics in Carbon-13 NMR Spectroscopy*; Levy, G. C., Ed.; John Wiley and Sons: New York, 1979; Vol. 3, Chapter 4, p 284.
- (14) Schaefer, J.; Stejskal, E. O. Buchdahl, R. *Macromolecules* **1977**, *10*, 384.
- (15) Sefcik, M. D.; Schaefer, J.; Stejskal, E. O.; McKay, R. A. *Macromolecules* **1980**, *13*, 1132.
- (16) Yannoni, C. S. *Acc. Chem. Res.* **1982**, *15*, 201.
- (17) Lyster, J. R.; Levy, G. C. Carbon-13 Nuclear Spin Relaxation. In *Topics in Carbon-13 NMR Spectroscopy*; Levy, G. C., Ed.; John Wiley and Sons: New York, 1974; Vol. 1, Chapter 3, p 79.
- (18) Harris, R. K. *Nuclear Magnetic Resonance Spectroscopy, A Physiological View*; Pitman: Marshfield, MA, 1983; Chapter 6.
- (19) Laupretre, F.; Monnerie, Virlet, J. *Macromolecules* **1984**, *17*, 1397.
- (20) Okamoto, D. T.; Copper, S. L.; Root, T. W. *Macromolecules* **1992**, *25*, 1068.
- (21) Craik, D. J.; Levy, G. C. Factors Affecting the Accuracy in ^{13}C Spin-Lattice Relaxation Measurements. In *Topics in Carbon-13 NMR Spectroscopy*; Levy, G. C., Ed.; John Wiley and Sons: New York, 1984; Vol. 4, Chapter 9, p 241.
- (22) Poliks, M. D.; Schaefer, J. *Macromolecules* **1990**, *23*, 2682.
- (23) Schaefer, J.; Stejskal, E. O. *J. Am. Chem. Soc.* **1976**, *98*, 1031.
- (24) Pines, A.; Gibby, M. G.; Waugh, J. S. *J. Chem. Phys.* **1973**, *59*, 569.
- (25) Frey, M. H.; Opella, S. J. *J. Am. Chem. Soc.* **1979**, *101*, 5854.
- (26) Garces, F. O.; Rao, V. P.; Garcia-Garibay, M.; Turro, N. J. *Supramol. Chem.* **1992**, *1*, 65.
- (27) Chang, C.; Muccio, D. D.; St. Pierre, S. *Macromolecules* **1985**, *18*, 2154.
- (28) Gupta, M. K.; Bansi, R. *J. Polym. Sci., Polym. Phys. Ed.* **1981**, *19*, 353.
- (29) Inoue, Y.; Fukutomi, T.; Chujo, R. *Polym. J.* **1983**, *15*, 103.
- (30) Lancaster, J. E.; O'Connor, M. N. *J. Polym. Sci., Polym. Lett. Ed.* **1982**, *20*, 547.
- (31) Muroga, Y.; Noda, I.; Nagasawa, M. *J. Phys. Chem.* **1969**, *73*, 667.
- (32) Schaefer, J. *Macromolecules* **1971**, *4*, 98.
- (33) Stehling, F. C.; Knox, J. R. *Macromolecules* **1975**, *8*, 595.
- (34) Pham, Q. T.; Petiaud, R.; LLauro, M.-F.; Waton, H. *Proton and Carbon NMR Spectra of Polymers*; John Wiley and Sons: New York, 1983; Vols. 1 and 2.
- (35) Fyfe, C. A.; McKinnon, M. S. *Macromolecules* **1986**, *19*, 1909.
- (36) Cheng, H. N.; Bennett, M. A.; *Anal. Chim. Acta* **1991**, *242*, 43.
- (37) Cheng, H. N. *Macromolecules* **1991**, *24*, 4813.
- (38) Cheng, H. N.; Babu, G. N.; Newmark, R. A.; Chien, J. C. W. *Macromolecules* **1992**, *25*, 6980.
- (39) Cheng, H. N.; Lee, G. H. *Polym. Bull.* **1984**, *12*, 463.
- (40) Gao, Y. P.; Zhou, Z. N.; Feng, Z. L. *Sci. China, Ser. B* **1990**, *33*, 777.
- (41) Lindeman, L. P.; Adams, J. Q. *Anal. Chem.* **1971**, *43*, 1245.
- (42) Chibowski, S. *J. Colloids Interface Sci.* **1990**, *140*, 444.
- (43) Bain, A. D.; Eaton, D. R.; Hamielec, A. E.; Mlekuz, M.; Sayer, B. G. *Macromolecules* **1989**, *22*, 3561.
- (44) Edzes, H. T.; Veeman, W. S. *Polym. Bull.* **1981**, *5*, 255.
- (45) Zhang, X.; Takegoshi, K.; Hikichi, K. *Macromolecules* **1991**, *24*, 2756.
- (46) Hmamouchi, M.; Lavellee, C.; Prud'homme, R. E.; Leborgne, A.; Spassky, N. *Macromolecules* **1989**, *22*, 130.
- (47) Zhang, X.; Natansohn, A.; Eisenberg, A. *Macromolecules* **1990**, *23*, 412.
- (48) Curran, S. A.; LaClair, C. P.; Aharoni, S. M. *Macromolecules* **1991**, *24*, 5903.